

BRDF MEASUREMENTS OF URBAN SURFACE MATERIALS AT THE EGO FACILITY USING A LASER SOURCE

André ROTHKIRCH, Gerhard MEISTER, Hartwig SPITZER, Johann BIENLEIN

CENSIS, II. Institute for Experimental Physics, University of Hamburg, Germany
Mail: c/o KOGS, FB Informatik, Vogt-Koelln-Str. 30, D-22527 Hamburg, Germany
www: <http://kogs-www.informatik.uni-hamburg.de/projects/censis/remotesens.html>
Email: rothkirc@informatik.uni-hamburg.de

KEY WORDS: BRDF, Laser, EGO Goniometer, Polarization, Diffuse scattering.

ABSTRACT

In this paper we present a study of the BRDF characteristics of urban surface materials (e.g. roof coverings). Multiangular measurements were made at the European Goniometer Facility, Ispra, Italy. We used a linearly polarized HeNe-laser as illumination source and a spectroradiometer with a mounted polarizer as detector. Measurements were done at horizontal (*s*) and vertical (*p*) polarisation states relative to the principal plane, resulting in measurements at four different combinations of source and detector orientation (*ss*, *sp*, *ps* and *pp*). We performed a systematic study of the accuracy of BRDF measurements to determine measured deviations from the Lambertian case. Polarization effects in the principal plane are analyzed for roof covering materials as well as for a Spectralon sample of 50% reflectance. The measurements show that the reflectance from our surface materials is a combination of different components. As a first approximation they can be described by a component due to internal scattering (diffuse component) and a component that is due to specular reflection of inclined surface facets.

1 INTRODUCTION

Remotely sensed multitemporal images allow, for example, analyses of urban infrastructure using computer based change detection (Wiemker et al., 1997), (Wiemker, 1997a). Usually, the images are taken at different illumination conditions (i.e. different incident sun zenith angle) and observation geometries which is why a transformation of the measured radiances into reflectances is done commonly using atmospheric radiative transfer models to be independent of such influences. Change detection is furthermore complicated by non-lambertian scattering characteristics, i.e. the intensity of the reflected radiance depends on the viewing geometry and is not only a function of the cosine of the incident irradiance. The directional dependencies of light reflected from a surface are described by the Bidirectional Reflectance Distribution Function BRDF as defined by (Nicodemus, 1970).

As part of our research program we conducted measurements of the BRDF of urban surface materials using laboratory and field measurements as well as airborne multispectral imagery ((Meister et al., 1998a), (Meister et al., 2000), (Meister et al., 1999), (Rothkirch et al., 1998)). In this paper we present results of laboratory BRDF measurements using polarized light.

2 MEASUREMENTS

Measurements were made at the EGO Goniometer at the Joint Research Centre, Ispra, Italy. We used a beam expanded, linearly polarized HeNe-laser at a wavelength $\lambda = 632$ nm as illumination source. A SE590 spectroradiometer (Spectron Eng., 1987a) with a mounted polarizer was used as detector. Measurements were done at horizontal (*s*) and parallel (*p*) polarisation states, yielding measurements at four different combinations of source and detector orientation (*ss*, *sp*, *ps* and *pp*).

2.1 Instrumentation

The EGO Goniometer is illustrated in fig. 1. Two quarter-arcs are mounted on a base azimuth arc of about 4 m diameter. The arc carrying the source is fixed in azimuth, the detector arc can be moved covering most azimuth positions. Source and detector can be moved in zenith angle (source up to 65° , detector up to 70°). A full description of the setup has been given by (Koechler, 1994). Sensitivity studies using unpolarized light have been reported by (Solheim et. al., 1996) and (Sandmeier et al., 1997).

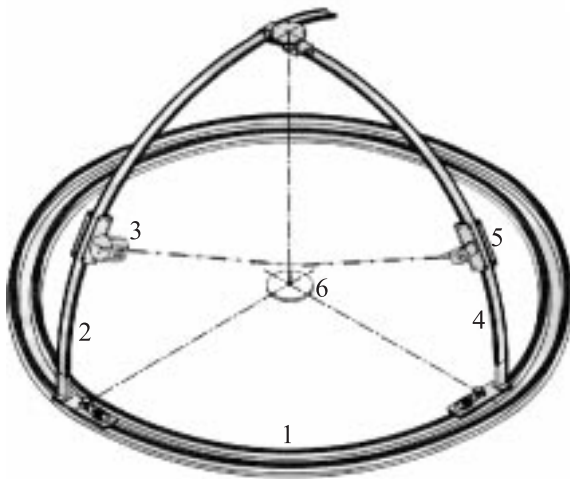


Figure 1: EGO Goniometer at the Joint Research Centre, Ispra, Italy. In the sketch of the instrument on the left the numbers indicate: 1) horizontal rail, 2 + 4) vertical quarter-arc, 3) light source, 5) detector, 6) target support. On the right you can see the author preparing the sample 'roof tile'. In the back of the right image you can see the two quarter-arcs with mounted detector (left, $\theta_r = 70^\circ$) and source (right, $\theta_i = 30^\circ$).

2.2 Measured BRDF values

In this section we present the measurements made in the 'principal plane', this means measurements with a relative azimuth angle between source and detector of 0° or 180° . While the detector zenith angle was varied across the principal plane, source zenith angles¹ were chosen to $\theta_i = 30^\circ, 45^\circ, 55^\circ, 65^\circ$. Measurements were done for roof covering materials (a roof tile made of baked clay and a sample of roofpaper made of sand and bitumen) as well as for a Spectralon (Labsphere Inc.) sample of 50 % reflectance (a description of the Spectralon can be found in (Meister et al., 1996)). BRDF values f_r were calculated from the ratio of the reflected L_r radiance and the incident irradiance E_i . The accuracy of the measured values was determined to $\sigma_{f_r} / f_r \approx 4.3\%$, a detailed description can be found in (Rothkirch et al., 1999).

Fig. 2 shows the measured BRDF values of the different surface materials across the principal plane. Each column gives the measured values of a surface depending on viewing zenith angle θ_r at different illumination angles $\theta_i = 30^\circ, 45^\circ, 55^\circ$ and 65° . The solid lines indicate measurements at polarization state *ss* (sample illuminated by *s* polarized light and detection of reflected light at polarization state *s*), the dashed lines indicate *sp*, the crosses show *pp*-measurements and the plus-signs show *ps*-measurements. Negative viewing zenith angles correspond to backward scattering direction.

It can be seen that all sample surfaces show a specular peak at the *ss*-measurements which increases with increasing incident zenith angle θ_i . For example the ratio q_{ss} between maximum and minimum BRDF value of the sample 'Red roof tile' rises from $q_{ss} \approx 3$ at $\theta_i = 30^\circ$ up to $q_{ss} \approx 12$ at $\theta_i = 65^\circ$. The specular peak is shifted towards greater viewing zenith angles θ_r (to $\theta_r \geq 70^\circ$ for all *ss* measurements). The *pp*-measurements also show a specular peak which increases with increasing incident zenith angle θ_i , but much weaker as compared to the *ss*-measurements. Similar results were found for a Spectralon panel with 100 % reflectance by (Haner et al., 1999). For the sample 'Red roof tile' its maximum ratio is $q_{pp} \approx 3$ at $\theta_i = 65^\circ$. At the *pp*-measurements of the sample 'Red roof tile' there is an increased reflection around a viewing angle of $\theta_r \approx 25^\circ$. While it is dominating at an incident zenith angle $\theta_i = 30^\circ$, it seems to vanish at $\theta_i = 55^\circ$ (unfortunately the field of view of the detector was too small to give reasonable results for measurements at $\theta_i = 65^\circ$ and low viewing zenith angles).

It also can be seen that there is a significant difference of the absolute height of the BRDF values between the measurements at different polarization states. Comparing the *ss*- and *pp*-polarization measurements of the sample 'Red roof tile', one can see that while in backward scattering direction the BRDF values are ≈ 0.04 [1 / sr] for *ss*-measurements, the values for *pp*-measurements are greater by ≈ 0.015 [1 / sr] (see also fig. 3). Every sample surface also shows different absolute BRDF values at cross polarization measurements (*sp* resp. *ps*).

While the samples 'Spectralon' and 'Red roof tile' only show significantly increasing specular reflection in forward scattering direction, a noticeable increase in backscatter direction can be seen for the sample 'sanded roof paper'. This is due to the sample structure: the sample consists of bitumen sparsely covered by sand. Hence if one looks from nadir onto the sample one can see the low reflective bitumen as well as the brighter sand. With increasing viewing zenith angle masking effects decrease the visible portion of bitumen until only sand can be seen. Assuming rotational symmetry of the sample surface one expects that a portion of the overall BRDF rises with increasing viewing zenith angle. Although this

¹A zenith angle $\theta = 0^\circ$ corresponds to nadir. In the sketch of the instrument (see fig. 1), detector angle θ_r and source zenith angle θ_i are $\approx 60^\circ$.

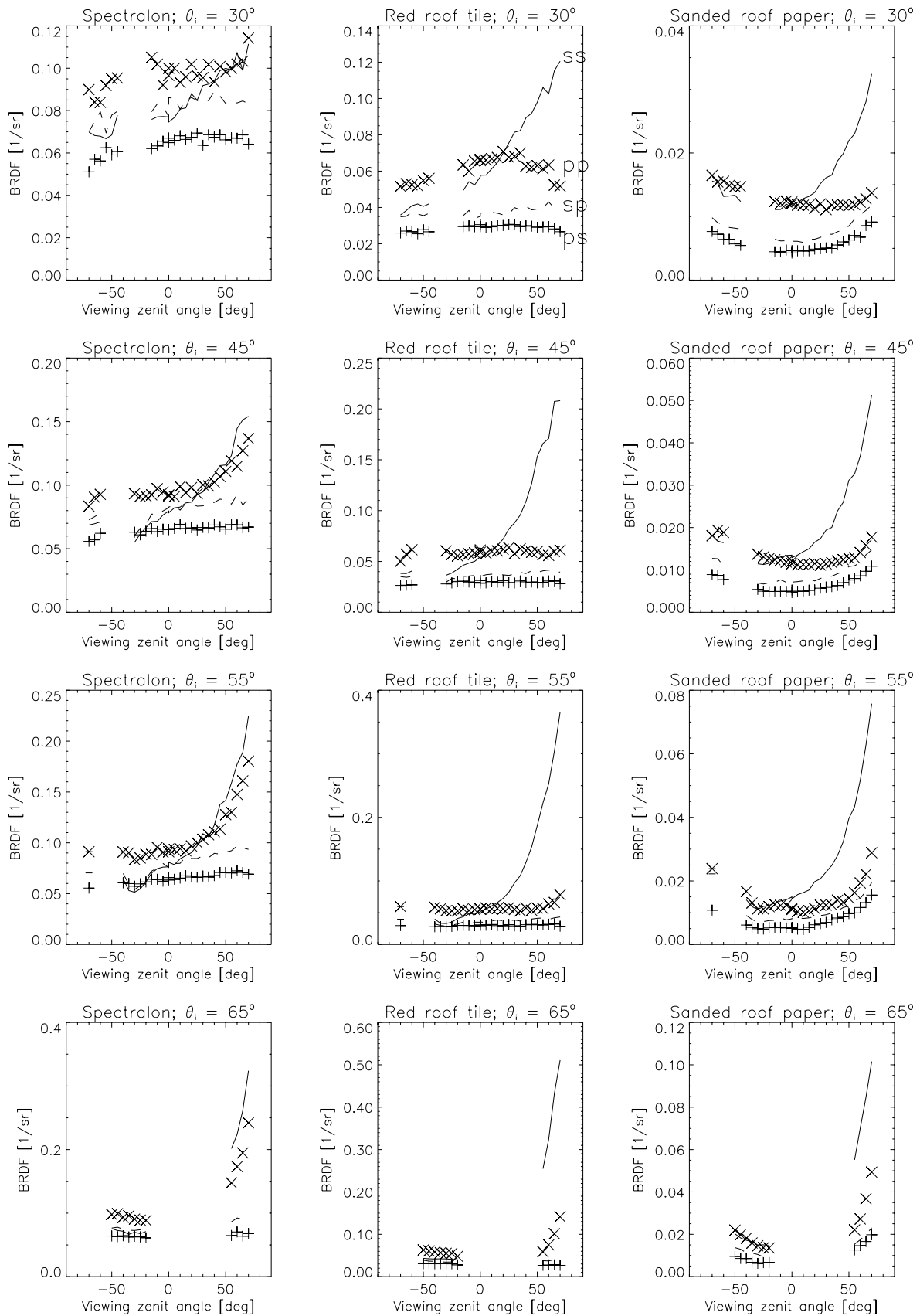


Figure 2: Measured BRDF values of different surface materials in the principal plane. Each column gives the measured values of a surface depending on viewing zenith angle θ_r , at different illumination angles θ_i . The solid lines indicate measurements at polarization state *ss*, the dashed lines indicate *sp*, the crosses show *pp*-measurements and the plus-signs show *ps*-measurements. Negative viewing zenith angles correspond to backward scattering direction. At $\theta_i = 65^\circ$ the used field of view was too small to give reasonable results at low viewing angles θ_r .

assumption is supported by the symmetry of the cross polarization measurements, this sample is not investigated in this study because the model of Torrance & Sparrow (see sec. 3) assumes lambertian reflection for the diffuse component.

3 BRDF MODEL OF TORRANCE & SPARROW

(Torrance et al., 1967) proposed a BRDF model in which they assumed that the surface consists of specularly reflecting V-cavities of infinite length. The distribution of the inclinations of the surface elements is assumed to be Gaussian, which results in a specular peak of Gaussian shape. For rough surfaces, this peak is shifted towards larger zenith angles. The model depends on the Fresnel reflectance F which is a function of the complex index of refraction $\hat{n} = n + ik$ and the angle of incidence (with respect to the reflecting surface element) and depends on polarisation. A 'Geometric-Attenuation-Factor' G accounts for effects of masking and shadowing, which become more important with larger zenith angles (Meister et al., 2000a). Because of the width of the specular peaks, G was not neglected as proposed in (Meister et al., 2000a)). The modeled BRDF values f_r are given by:

$$f_r = a_0 + a_1 \cdot \frac{F(\theta_i, \theta_r, \phi, \hat{n}) G(\theta_i, \theta_r, \phi)}{\cos \theta_i \cos \theta_r} \cdot e^{-a_2 \alpha^2} \quad \left[\frac{1}{\text{sr}} \right], \quad (1)$$

where $\alpha = \alpha(\theta_i, \theta_r, \phi)$ is the angle between nadir and the normal of the specularly reflecting surface element (unit is [degree]). a_0 is a constant which gives the diffuse component, a_1 is determining the intensity of the specular reflection and a_2 is describing the width of the specular peak. We interpret the diffuse component to be due to *multiple or internal* scattering and not due to specular reflection. This means that if a sample surface shows differences in the intensity of the specular peak at different polarization states (s or p), different portions of intensity can contribute to multiple scattering and we expect different values of the diffuse component a_0 . We therefore fitted the model given by eq. 1 to ss - and pp -measurements using two coefficients a_0^{ss}, a_0^{pp} to describe the diffuse component (one for each polarization orientation). Coefficients a_1, a_2 and \hat{n} were chosen to be the same for both measurements. Resulting coefficients are given in tab. 1 for the samples 'Spectralon' and 'Red roof tile'.

Figures 3 and 4 show the measured BRDF values of the samples 'Spectralon' and 'Red roof tile', indicated by the error-bars. The first row in fig. 3 shows the measured values of 'Spectralon' at different incident zenith angles θ_i at polarization state ss , the second row gives the results at polarization state pp . The lower two rows give the results for the sample 'Red roof tile'. The solid line gives the result from the fit² of the model to the data when the diffuse components a_0^{ss}, a_0^{pp} were fitted separately for each sample. It can be seen that the model is able to describe the specular reflection of the 'Red roof tile' very well for ss - and pp -polarization. It describes the strong specular behavior at ss -polarization as well as the much weaker specular reflection at pp -polarization which are both shifted to large viewing zenith angles. It also covers an increased reflection at low viewing zenith angles. For the sample 'Spectralon' one can see stronger deviations between model and measurements. The model roughly describes the reflection properties, but cannot give the real shape. Better results might be obtained with a different distribution of the surface facets. Nevertheless modelling results are in far better agreement with measurement results than the lambertian assumption.

Figure 4 gives the results for the cross-polarization measurements. As a first approximation the solid line gives the result of a lambertian assumption (separately fitted constants a_0^{sp}, a_0^{ps} to each sample). Resulting coefficients are also given in table 1. At cross-polarization the deviations from lambertian for s -polarized incident light are 9 % for 'Spectralon' and 4.9 % for 'Red roof tile' on average. At p -polarized incident light the deviations are 6.2 % for 'Spectralon' and 4.2 % for 'Red roof tile' on average. In the first and third row of fig. 4 you can see a local minimum at viewing zenith angles between about -10° and -40° . We expect this to be caused by the fact that the detector field of view did not cover the whole illuminated sample area in that source and detector position. Similar effects were found by a comparison of measurements where different fields of view were used. This needs further investigation. The dashed line gives the result of a fit to a constant when the measured BRDF values at viewing zenith angles between -10° and -40° were neglected.

An interesting result can be obtained by a summation of the contributions at fixed incident polarization state. The total albedo ρ_x for incident light at a polarization state x is given by

$$\rho_x = a_{0xx} \cdot \pi + a_{0xy} \cdot \pi + \bar{I}_{xx}^{\text{spec}}, \quad (2)$$

when y denotes the corresponding cross-polarization state and $\bar{I}_{xx}^{\text{spec}}$ is the contribution from specular reflection averaged over the four incident zenith angles $\theta_i = 30^\circ, 45^\circ, 55^\circ$ and 65° as used in the measurements. $\bar{I}_{xx}^{\text{spec}}$ as a function of the

²Minimizing $\sum_{i=1}^N \left(\frac{M_i - f_i}{\sigma_{f_i}} \right)^2$, where N is the number of ss - and pp -measurements, M_i denotes the i -th value obtained from the model and f_i the corresponding measured BRDF value f_i with accuracy σ_{f_i} .

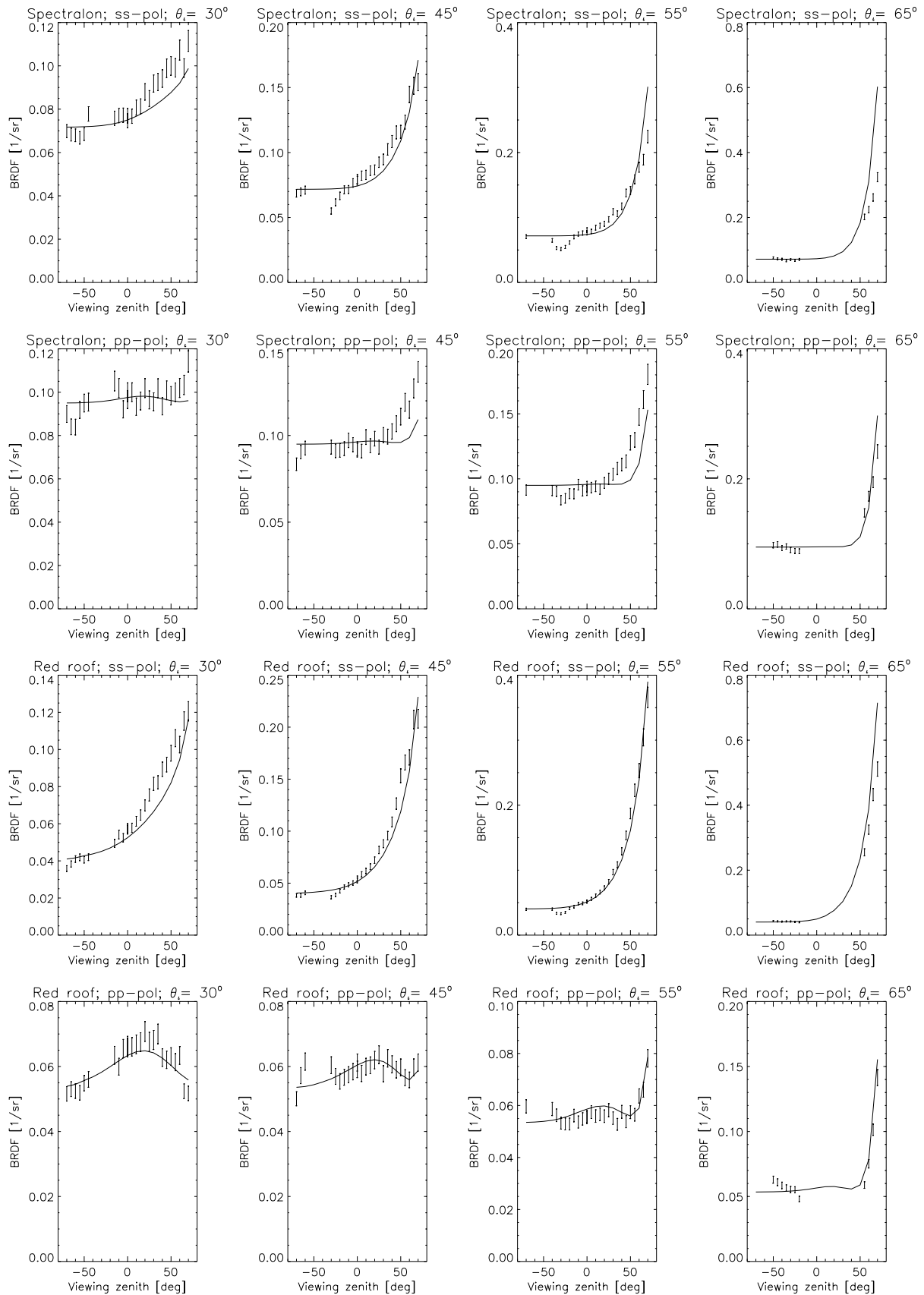


Figure 3: Measured BRDF values in the principal plane at like-polarization. Within a row the incident zenith angle θ_i was varied, the rows differ in measured polarization state (*ss* resp. *pp*) and measured sample. Measurements are indicated by error-bars, the solid line gives the result from the fit to the model (coefficients see table 1). Negative viewing zenith angles correspond to backward scattering direction.

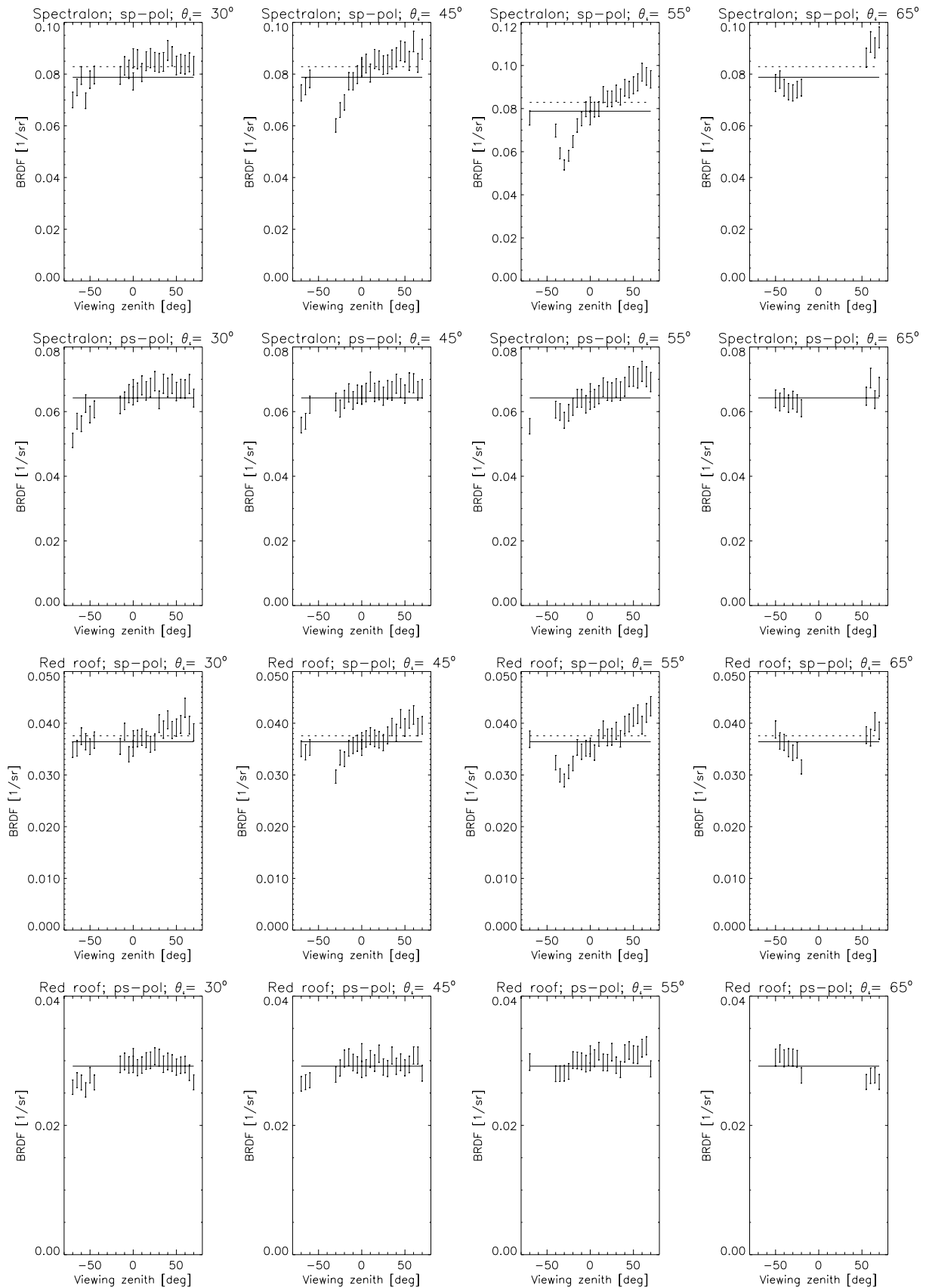


Figure 4: Measured BRDF values in the principal plane at cross-polarization. Within a row the incident zenith angle θ_i was varied, the rows differ in measured polarization state (*sp* resp. *ps*) and measured sample. Measurements are indicated by error-bars, the solid line gives the result of a lambertian assumption (separately fitted constants a_0^{sp} , a_0^{ps} for each sample). Negative viewing zenith angles correspond to backward scattering direction.

Sample	Polarization	a_0 [$\frac{1}{\text{sr}}$]	a_1 [$\frac{1}{\text{sr}}$]	a_2 [$\frac{1}{\text{degree}}$]	n	k
Spectralon	<i>ss</i>	0.072	0.53	0.048	1.03	0.18
	<i>pp</i>	0.095	0.53	0.048	1.03	0.18
	<i>sp</i>	0.079	-	-	-	-
	<i>ps</i>	0.064	-	-	-	-
Red roof tile	<i>ss</i>	0.040	0.40	0.038	1.35	0.25
	<i>pp</i>	0.053	0.40	0.038	1.35	0.25
	<i>sp</i>	0.036	-	-	-	-
	<i>ps</i>	0.029	-	-	-	-

Table 1: Coefficients to describe the given samples by the model of Torrance & Sparrow. Note that the diffuse components a_0^{ss} , a_0^{pp} , a_0^{sp} and a_0^{ps} were fitted separately.

incident zenith angle is given by the integral of the specular peak over the viewing angles ω given by the upper hemisphere Ω :

$$I_{\text{spec}}^{xx}(\theta_i) = \int_{\Omega} a_1 \cdot \frac{F(\theta_i, \theta_r, \phi, \hat{n}) G(\theta_i, \theta_r, \phi)}{\cos \theta_i \cos \theta_r} \cdot e^{-a_2^2 \alpha^2} d\omega \quad (3)$$

With parameters from tab. 1 results are:

$$\begin{aligned} \rho_s^{\text{Spectralon}} &\approx (0.072 + 0.079) \cdot \pi + 0.023 = 0.497 \\ \rho_p^{\text{Spectralon}} &\approx (0.095 + 0.064) \cdot \pi + 0.004 = 0.504 \\ \rho_s^{\text{Red roof tile}} &\approx (0.040 + 0.036) \cdot \pi + 0.068 = 0.307 \\ \rho_p^{\text{Red roof tile}} &\approx (0.053 + 0.029) \cdot \pi + 0.012 = 0.272 \end{aligned}$$

The difference of the albedos is below 1.5 % for Spectralon and below 13 % for the 'Red roof tile'. The contributions from the specular albedo to the total albedo $\Delta_x = \overline{I_{xx}^{\text{spec}}} / (a_{0xx} \cdot \pi + a_{0xy} \cdot \pi)$ are $\Delta_s \approx 5$ % and $\Delta_p \approx 1$ % for the Spectralon sample and $\Delta_s \approx 28$ % and $\Delta_p \approx 5$ % for the sample 'Red roof tile'. An accurate reproduction of the specular peak is therefore more important for the sample 'Red roof tile' than for the Spectralon sample.

Also noticeable is that for the Spectralon sample the given albedos are close to the albedo determined by a calibration by the manufacturer of $\rho_{\text{Fab}} = 0.511$ (Labsphere Inc., 1994).

4 SUMMARY AND OUTLOOK

BRDF measurements of urban surface materials made with a linearly polarized HeNe-laser as illumination source were presented. Polarization effects in the principal plane were analyzed for a roof tile as well as for a Spectralon sample of 50% reflectance. Both samples show different reflection properties with respect to the polarization states *ss*, *pp*, *sp* and *ps*. At *ss*-polarization the samples show a strong specular peak which increases with increasing incident zenith angle and which is shifted towards greater viewing zenith angles. At *pp*-polarization the specular reflection is much weaker as compared to *ss*-polarization. In contrast cross polarization measurements (*sp* resp. *ps*) show almost lambertian reflection. The BRDF values also differ absolutely with respect to polarization states.

It was shown that the reflectance from our surface materials can be described by the model of Torrance & Sparrow (Torrance et al., 1967). The reflection of the samples can be interpreted as a combination of a diffuse component (internal scattering) and a component that is due to specular reflection of statistically distributed surface facets. The model reproduces the specular behavior of the samples. Cross polarization measurements of the samples 'Spectralon' and 'Red roof tile' can be described by a lambertian assumption within deviations of 6.1 % on average. Absolute Differences of the cross- and like-polarized diffuse components are about 10 % at *s*-polarized incident light and about 39 % at *p*-polarized incident light on average. Differences of the total albedo for *s*- and *p*-polarized incident light are within 1.5 % for Spectralon and below 13 % for the 'Red roof tile'.

Acknowledgements

We would like to thank our colleagues of our working group and the coworkers of the Dep. for Computer Science for their support and fruitful discussions. The measurement campaign was performed in collaboration with the Joint Research Center (JRC), Ispra, Italy. We acknowledge the contributions particularly of B. Hosgood and G. Andreoli from JRC.

REFERENCES

- Haner D. A., McGuckin B. T., Bruegge C.J., Polarization characteristics of Spectralon illuminated by coherent light, *Applied Optics*, Vol. 38, No. 30, pp. 6350-6356.
- Koechler C., Hosgood B., Andreoli G., Schmuck G., Verdebout J., Pegoraro A., Hill J., Mehl W., Roberts D. and Smith M., 1994. The European Optical Goniometric Facility: Technical Description and First Experiments on Spectral Unmixing. Proc. of IGARSS'94, Pasadena.
- Labsphere Inc., Calibration certificate SRT-50-120, Report No. 12611-D, Labsphere Inc., P.O.Box 70, North Sutton, NH 03260, Nov. 1994
- Meister G., Wiemker R., Bienlein J., Spitzer H., In Situ Measurements of Selected Surface Materials to Improve Analysis of Remotely Sensed Multispectral Imagery, Proceedings of the XVIII. Congress of the International Society for Photogrammetry and Remote Sensing ISPRS, 1996, Vienna, Vol. XXXI part B7 of International Archives of Photogrammetry and Remote Sensing, p.493 - 498, 1996.
- Meister G., Rothkirch A., Wiemker R., Bienlein J. and H. Spitzer, Modeling the Directional Reflectance (BRDF) of a Corrugated Roof and Experimental Verification, Proceedings of the International Geoscience and Remote Sensing Symposium IGARSS'98, Seattle, IEEE, Vol. III, pp. 1487-1489, 1998
- Meister G., Wiemker R., Monno R., Spitzer H. and Strahler A., Investigation on the Torrance-Sparrow Specular BRDF Model, Proceedings of the International Geoscience and Remote Sensing Symposium IGARSS'98, Seattle, IEEE, Vol. IV, pp. 2095-2097, 1998
- Meister G., Lucht W., Rothkirch A., Spitzer H., Large Scale Multispectral BRDF of an Urban Area, Proceedings of the International Geoscience and Remote Sensing Symposium IGARSS'99, Hamburg, IEEE, Vol. II, pp. 821-823, 1999
- Meister G., Rothkirch A., Spitzer H. and Bienlein J., Large Scale Bidirectional Reflectance Model for Urban Areas, submitted to *Remote Sensing of Environment*, 2000
- Meister G., Rothkirch A., Spitzer H. and Bienlein J., The shape of the specular peak of rough surfaces, Proceedings of ISPRS2000, Amsterdam, this issue
- Nicodemus F.E., Reflectance Nomenclature and Directional Reflectance and Emissivity, *Applied Optics*, 9(6), pp. 1474-1475, 1970
- Rothkirch A., Kollwe M., Spitzer H., Calibration accuracy of aerial multispectral reflectance images and estimation of error sources, Proceedings of the 1st workshop on imaging spectroscopy, Zurich, CH, ISBN 2-90885-22-0, pp. 155-163, 1998
- Rothkirch A., Meister G., Hosgood B., Spitzer H. and Bienlein J., BRDF Measurements at the EGO using a Laser Source: Equipment characteristics and estimation of error sources, Second International Workshop on Multiangular Measurements and Models (IWMMM-2), Ispra, Italy, 1999 (submitted to *Remote Sensing Reviews*)
- Sandmeier S., Müller C., Hosgood B. and Andreoli G., 1997, Sensitivity Studies of Bidirectional Reflectance Data using the EGO/JRC Goniometer Facility, 7th Int. ISPRS Symposium on Physical Measurements and Signatures in Remote Sensing, Courchevel, France, April 6-11, pp. 351-356, Balkema Publ. NL, ISBN 90 5410 918 1
- Solheim I., Hosgood B., Andreoli G. and Piironen J., Calibration and Characterization of Data from the European Goniometer Facility (EGO), Joint Research Centre European Commission, EUR 17268 EN, 1996
- Spectron Engineering, Operating manual - SE590 field-portable data-logging spectroradiometer, 800 West 9th avenue, Denver, Colorado 80204, USA, 1987
- Torrance K. and Sparrow E., Theory for off-specular reflection from rough surfaces, *Journal of the Optical Society of America*, Vol. 57, No. 9, pp. 1105-1114, 1967
- Wiemker R., Speck A., Kulbach D., Spitzer H., Bienlein J., Unsupervised Robust Change Detection on Multispectral Imagery Using Spectral and Spatial Features, Proceedings of the Third International Airborne Remote Sensing Conference and Exhibition, Copenhagen, July 1997, vol. I, p.640-647. ERIM, Ann Arbor 1997.
- Wiemker R., Unsupervised Fuzzy Classification of Multispectral Imagery Using Spatial-Spectral Features, Data Highways and Information Flooding, a Challenge for Classification and Data Analysis, Proceedings of the 21. Annual Meeting of the Gesellschaft für Klassifikation, GfKI'97, Potsdam, March 12-14, Springer, Heidelberg, 1997